Australian Journal of Earth Sciences
Publication details, including instructions for authors and subscription information:
http://www.informaworld.com/smpp/title~content=t716100753

The genesis of Pb-Zn sulphide occurrences in the Lower Devonian Buchan Group, Victoria

D. C. Arne [a b]; P. W. Cromie [a c]; J. A. Webb [d]; J. R. Richards [e]
[a] School of Earth Sciences, University of Melbourne, Parkville, Vic., Australia [b] Department of Earth Sciences, Dalhousie University, hali, Nova Scotia, Canada [c] BHP Iron Ore, Newman, WA, Australia [d] Department of Geology, La Trobe University, Bundoora, Vic., Australia [e] Research School of Earth Sciences, Australian National University, Canberra, ACT, Australia

Online Publication Date: 01 April 1994

To cite this Article Arne, D. C., Cromie, P. W., Webb, J. A. and Richards, J. R.(1994)'The genesis of Pb-Zn sulphide occurrences in the Lower Devonian Buchan Group, Victoria',Australian Journal of Earth Sciences,41:2,75 — 90

To link to this Article: DOI: 10.1080/08120099408728117

URL: http://dx.doi.org/10.1080/08120099408728117

Australian Journal of Earth Sciences (1994) **41**, 75–90

The genesis of Pb–Zn sulphide occurrences in the Lower Devonian Buchan Group, Victoria

D. C. ARNE,[1*] P. W. CROMIE,[1†] J. A. WEBB[2] AND J. R. RICHARDS[3]

[1] *School of Earth Sciences, University of Melbourne, Parkville, Vic. 3052, Australia.*
[2] *Department of Geology, La Trobe University, Bundoora, Vic. 3083, Australia.*
[3] *Research School of Earth Sciences, Australian National University, Canberra, ACT 0200, Australia.*

Six minor sulphide occurrences hosted by the Lower Devonian Buchan Group have been investigated. Sulphide minerals and associated phases are hosted by both dolostone and limestone lithologies along stylolitized bedding planes, cross-cutting fractures, low angle minor faults and in cavities. Mineralization was closely associated with minor structures of inferred Tabberabberan age (Middle Devonian), which it appears to have post-dated, but was largely strata-bound in nature. The mineralogy of the occurrences is simple and characterized by the following generalized paragenesis which reflects the increasing oxidation state and pH of the mineralizing fluids: pyrite (pseudomorphous after marcasite)–galena ± sphalerite ± pyrite–dolomite ± barite–calcite ± fluorite ± dolomite.

The sulphur isotope composition of sulphide minerals varies from –32.1 to +4.1‰, with iron and base metal sulphide minerals forming two distinct populations around –25‰ and 0‰, respectively. A single barite sample gives a sulphur isotope composition of +22.4‰, which is similar to that estimated for Early Devonian seawater. Fluid inclusions in fluorite and calcite homogenize at temperatures in the range 160 to 212°C and have average salinities of approximately 10 wt% NaCl eq. Sphalerite contains up to 1.81 wt% iron which correlates with colour, and up to 1.43 wt% cadmium. The Pb isotopic pattern of galena suggests a source region with U/Pb ($= \mu$) lower than the crustal average, and a high Th/U.

A genetic hypothesis is proposed which involves the circulation of saline fluids through the Snowy River Volcanics, which directly underlie the Buchan Group, during or at some time after the Tabberabberan Orogeny. Although the Buchan occurrences show features characteristic of both Mississippi Valley-type and stratiform ore deposits, they are most directly comparable to the epigenetic zones of Irish carbonate-hosted base-metal deposits. However, Pb–Zn sulphide mineralization at Buchan appears to have been associated with minor compressional structures, suggesting that a simple correlation with the Irish deposits is not directly applicable.

Key words: Buchan Group, Devonian, ore genesis, Pb–Zn sulphide minerals.

INTRODUCTION

Minor occurrences of Pb, Zn and Ag are hosted by the Buchan Group in eastern Victoria (Fig. 1). Although not economically significant at the present, the occurrences were worked in the latter part of the 19th century and earlier this century, and the area has periodically been subjected to renewed exploration. However, the occurrences have received little detailed investigation and their genesis remains controversial.

In recent reviews O'Shea (1980) and Cochrane (1982) proposed conflicting genetic hypotheses for the occurrences. O'Shea (1980) equated the Buchan occurrences with stratiform base metal deposits and suggested a syngenetic style of mineralization followed by remobilization during subsequent tectonism. Cochrane (1982) considered the Buchan occurrences to be epigenetic in style and compared them favourably to carbonate-hosted base metal deposits of the Mississippi Valley-type.

In order to better constrain possible genetic models, a detailed investigation of the occurrences was undertaken. This study involved detailed mapping of several occurrences (Pyramids–Henham's, Back Creek, Spring Creek), petrographic and mineralogical descriptions of sulphide phases and their relationship to carbonate cements, fluid inclusion studies, sulphur isotope determinations and an evaluation of lead isotopes. The results of these studies are presented in the following sections. In the light of these new results a comprehensive model for mineralization is proposed and a critical comparison with various ore deposit types is made.

REGIONAL GEOLOGICAL SETTING

The extensive Lower Devonian sequence preserved in eastern Victoria includes the Snowy River Volcanics and the Buchan Group (Vandenberg 1988). The Snowy River Volcanics consist of a complex series of predominantly

*Present address: Department of Earth Sciences, Dalhousie University, Halifax, Nova Scotia, Canada, B3H 3J5.
†Present address: BHP Iron Ore, PO Box 655, Newman, WA 6753, Australia.

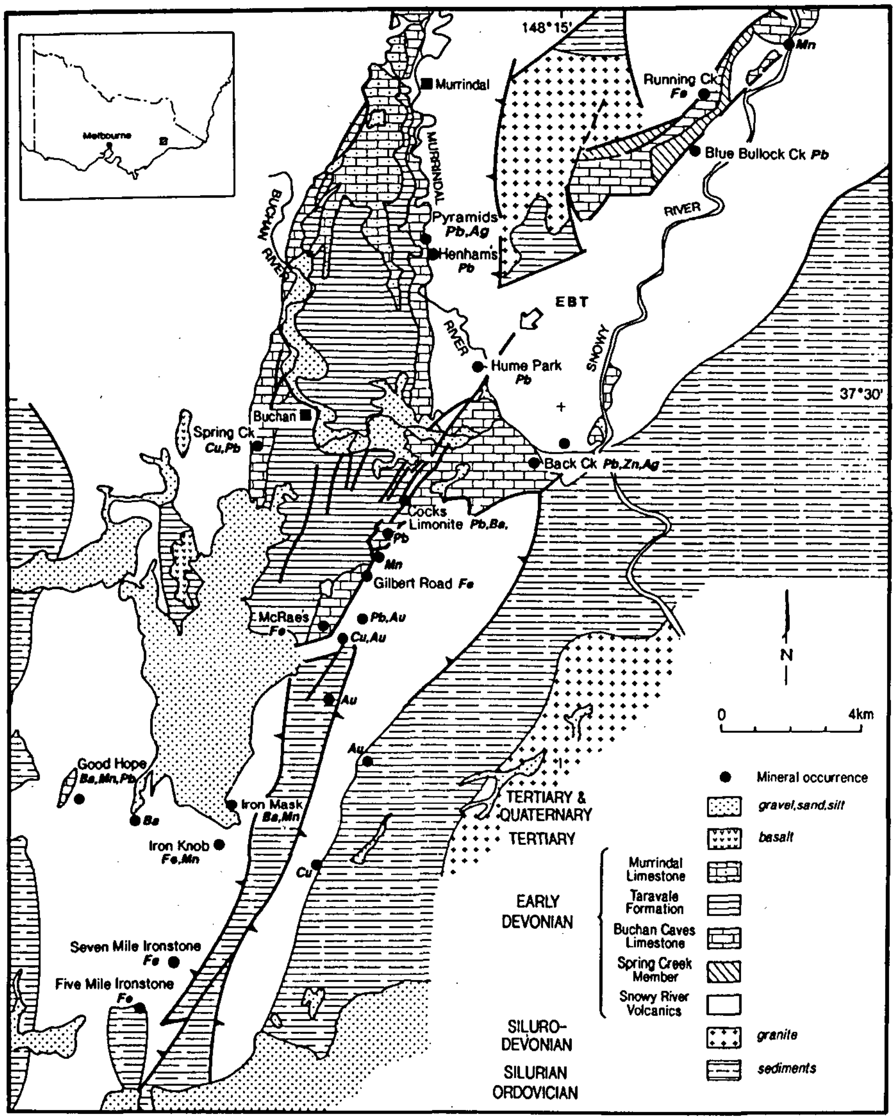

Fig. 1 Regional geological setting of the Buchan area. The positions of minor sulphide occurrences are also shown, including those hosted by the Buchan Caves Limestone. The position of the East Buchan Thrust (EBT) is also indicated. Note that the outcrop of inferred Murrindal Limestone at McRae's limonite deposit is too small to be shown at this scale. Map compiled by BHP-Utah Minerals International.

rhyolitic volcanic rocks that were deposited in a continental rift basin (Orth *et al.* 1989). In the Buchan area, the Snowy River Volcanics are overlain by the marine Buchan Group (Teichert & Talent 1958) which is preserved in a north-trending structural basin, the Buchan–Murrindal Synclinorium, that formed during the Tabberabberan Orogeny (Vandenberg & O'Shea 1981). A simplified geological map of the region is presented in Fig. 1.

The Buchan Group has been subdivided into three formations by Teichert and Talent (1958): Buchan Caves Limestone, Taravale Formation and Murrindal Limestone. The transition from terrestrial volcanism to marine carbonate sedimentation is marked by the Spring Creek Member at the base of the Buchan Caves Limestone. Immediately overlying the Spring Creek Member is approximately 40 m of extensively dolomitized limestone in which few fossils are recognizable (Husain 1981). The upper portion of the Buchan Caves Limestone becomes increasingly argillaceous until it grades into lime mudstone of the overlying Pyramids Marlstone Member of the Taravale Formation, which marks a transition from open-marine platform deposition to deeper water sedimentation. In the northern part of the synclinorium, deep-water sedimentation of the Pyramids Marlstone Member gave way to shallow marine deposition of the Murrindal Limestone. In total, a thickness of about 1100 m of Buchan Group is preserved in the southern Buchan–Murrindal Synclinorium, while nearly 700 m is preserved to the north.

Structural deformation during the Middle Devonian Tabberabberan Orogeny affected the Buchan Group in a variety of ways (Teichert & Talent 1958). Ductile deformation is indicated by a series of parasitic folds plunging gently to the south parallel to the axis of the main synclinorium. East–west compression during the Tabberabberan Orogeny was also accompanied by faulting along high and low angle thrust faults subparallel to bedding, the most significant of which is the East Buchan Thrust (Fig. 1), and by minor east-trending faults orientated at a high angle to bedding. These east–west trending faults occasionally offset the contact between dolostone and limestone in the Buchan Caves Limestone and therefore post-date dolomitization.

The morphological evolution of the Buchan region has recently been discussed by Webb *et al.* (1991). Cave systems formed during the Late Eocene to Early Oligocene are preserved in the Murrindal Limestone and similar cave systems developed in the Buchan Caves Limestone during the Late Tertiary. The youngest (?Pleistocene) caves in the area are extensive horizontal epiphreatic systems, which run parallel to bedding, at or slightly above current river levels (Webb *et al.* 1992). Late Tertiary cave systems are closely associated with mineralized strata at the Pyramids, Henham's, Hume Park and Back Creek occurrences, in that oxidized ore was mined from some of the caves. It should be noted that cave development at all localities clearly post-dates sulphide mineralization, and that many cave passages lack any association with sulphide minerals. However, the fact that all of the main occurrences are associated with cave systems suggests that the presence of sulphide minerals may have been conducive to cave formation. Sulphuric acid released during sulphide oxidation is likely to have been significant in this regard. As an example, the very extensive Carlsbad Caverns in New Mexico, U.S.A. were formed by sulphuric acid dissolution (Ford & Williams 1989).

DESCRIPTION OF OCCURRENCES

General

Minor occurrences of base and precious metals are found throughout the Lower Devonian sequence in eastern Victoria (Ramsay & Vandenberg 1986; Vandenberg 1988). Base metal sulphide occurrences hosted by the Buchan Group occur at two main horizons (O'Shea 1980; Cochrane 1982). The major sulphide occurrences are found predominantly within the basal dolostone of the Buchan Caves Limestone, while limonite crops out extensively within a limestone horizon equivalent to the Murrindal Limestone (Pype 1992).

Although many of the occurrences hosted by the Buchan Group have been mined intermittently over the last 120 years, little is known about the field relationships or the petrology and paragenesis of the sulphide minerals, as well as their relationship with carbonate cements. Therefore, in order to provide this basic information, detailed examinations were made of five occurrences, at Pyramids, Henham's, Back Creek, Hume Park, and Spring Creek (Fig. 1). The area around these occurrences was mapped in detail (Cromie 1990), with the exception of Hume Park which is poorly exposed. Detailed examinations were made of 25 hand samples, including reflected and transmitted light petrography, as well as cathodoluminescence and conventional carbonate staining techniques. As an example of the limonite occurrences, seven samples were examined from limestone hosting McRae's limonite deposit (Fig. 1). Details of all samples examined in the course of this investigation are given in Cromie (1990).

Pyramids and Henham's occurrences

The Pyramids and Henham's Pb–Ag occurrences are located on the west bank of the Murrindal River approximately 7 km to the northeast of Buchan (Fig. 1). A small amount of ore is believed to have been recovered from the Pyramids workings late last century, while the Henham's occurrence was worked as recently as the 1940s (Teichert & Talent 1958). Recent assays of gossanous material from the vicinity of the Henham's workings are reported at 0.5–6.5% Pb, 2.4–33% Zn and 42–195 g/t Ag (Cochrane 1982). Access to the abandoned workings at the Pyramids occurrence is via a series of cave entrances that have been enlarged by mining activity. The former Henham's workings consist of a main adit and numerous underlay shafts along the bank of the Murrindal River.

In this area a thickness of approximately 260–290 m of Buchan Caves Limestone is well exposed along the west bank of the Murrindal River (Fig. 2) and the basal 50–60 m is either pervasively or partially dolomitized. Bedding dips moderately to the west, with the contact between the base of the Buchan Caves Limestone and the Snowy River Volcanics generally following the river. Dolostone beds in the Pyramids workings are warped along a northwest-trending axis parallel to low angle reverse faults; the latter indicated within the former mine workings by the presence of slickenslides and grooved surfaces. Flexure and faulting were accompanied by intense fracturing of particular dolostone horizons and the introduction of an early non-luminescent sparry dolomite cement. Fine grained massive to coarsely crystalline galena, pyrite, and sphalerite occur as veins less than 30 mm in thickness along fault surfaces as well as in fractures and vugs that cross-cut the earliest generation of sparry dolomite veining. Galena replaces pyrite where the two phases are in contact.

Along the bed of the Murrindal River to the north of the Pyramids workings, purple fluorite crystals 1–3 mm across occur in carbonate cement-filled cavities up to 30 mm in diameter. These carbonate-filled cavities are lined from the margins inward by minor sphalerite, non-ferroan calcite, and saddle dolomite cement intergrown with fluorite. This zone is situated slightly below the strata-bound mineralized horizon in an area of limestone preserved at the base of the Buchan Caves Limestone, indicating that mineralization was not confined to dolomitized limestone.

At the Henham's workings, sulphide minerals occur along a single fractured horizon approximately 1 m thick subparallel to bedding in the host dolostone. Galena and iron sulphide minerals, the latter now extremely oxidized, occur along stylolites as veins 10–40 mm across. Where obliquely orientated veins intersect, galena is concentrated in irregular cavities. Both cerussite and smithsonite, indicated by a distinctive light blue and pink luminescence respectively, and confirmed by microprobe analyses, are common at both the Henham's and Pyramids occurrences. A more detailed description of the Henham's occurrence is not possible because of its highly oxidized nature.

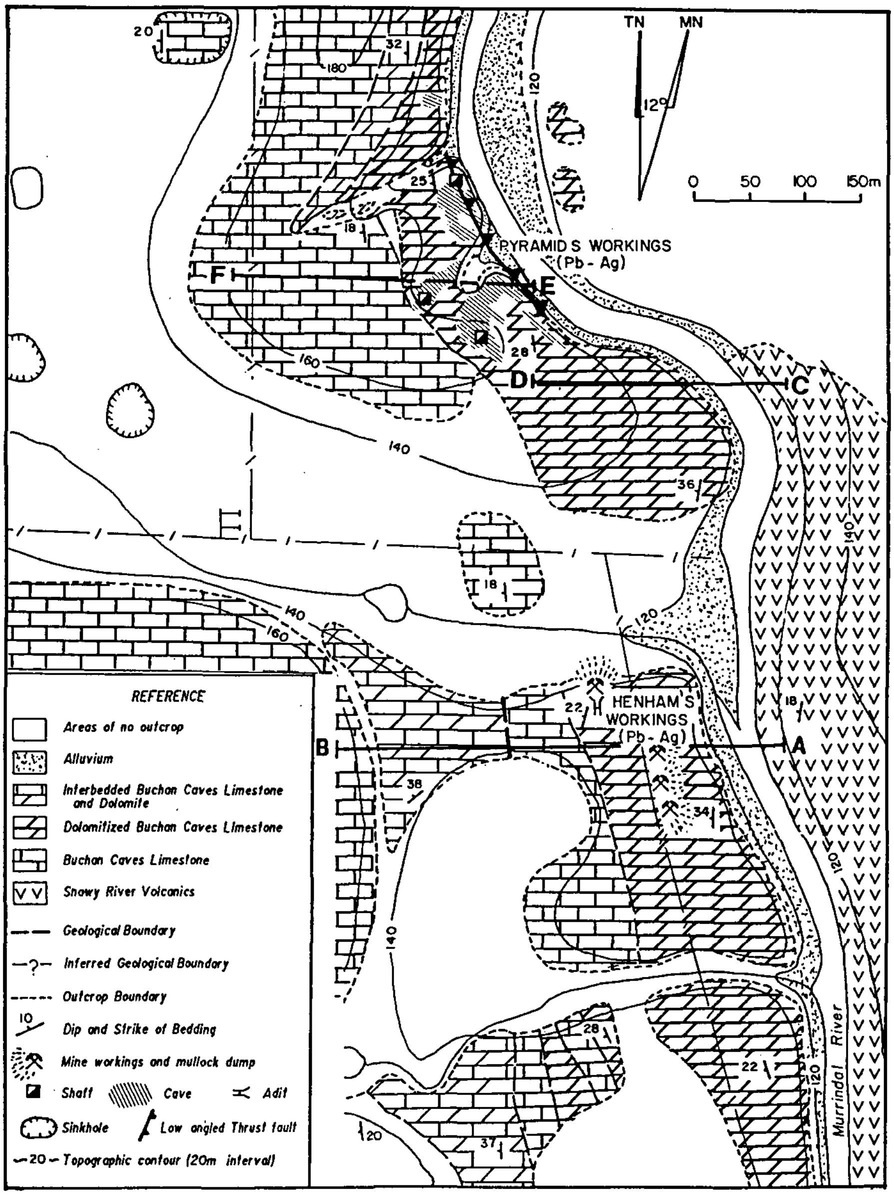

Fig. 2 Geological map showing the location of the Pyramids and Henham's occurrences (after Cromie 1990). A–F are the positions of measured stratigraphic sections presented in Fig. 7.

Back Creek occurrence

The Back Creek occurrence is situated approximately 7 km east of Buchan on both sides of Back Creek near its confluence with the Buchan River (Fig. 3). Lead ore was mined intermittently late last century (see Cochrane 1982). Much of the ore is reported to have been oxidized, and was presumably mined from cavern fill associated with a cave system into which the workings open. Several vertical shafts sunk in the area have been filled but access to the main workings may still be gained through several underlay shafts along the south bank of Back Creek.

The lower 90 m of the basal Buchan Caves Limestone in the area has been pervasively dolomitized. These beds are gently folded about a syncline axis that plunges shallowly to the north. The western boundary of the main workings is marked by an intensely weathered mafic (?) dyke approximately 60 cm thick that strikes north–south and dips steeply to the west. North of Back Creek the continuation of this dyke is offset 20 m to the east, suggesting that the creek is underlain by a fault. A strongly foliated zone containing laminated calcite veins along the eastern contact indicates that faulting has also affected the dyke. The age of this dyke is not known, but it is inferred to be pre-Tabberabberan as it is deformed and offset by presumed Tabberabberan structures.

Sulphide minerals at Back Creek are restricted to a single horizon approximately 1.5 m thick situated 26 m above the base of the Buchan Caves Limestone. Within this horizon, galena with minor pyrite, sphalerite, and chalcopyrite occur along narrow veins up to 1 cm thick both subparallel and oblique to bedding, and as lenses and cavity fillings. This mineralized horizon can be traced along the eastern limb of the syncline but does not extend

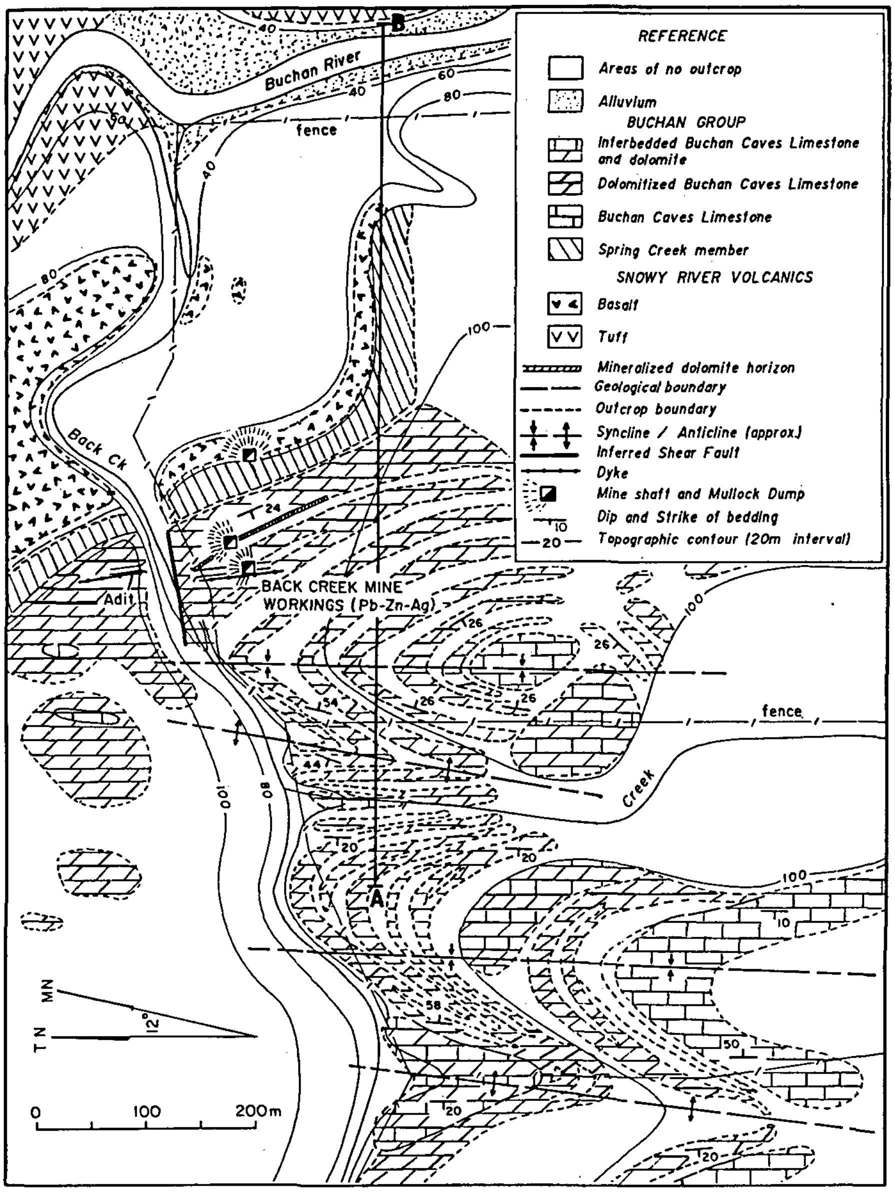

Fig. 3 Geological map showing the location of the Back Creek occurrence (after Cromie 1990). A–B is the position of the measured stratigraphic section shown in Fig. 7.

beyond the dyke. Rare pyrite veinlets cross-cut both the dyke and foliated material at the intrusive contact. Thus sulphide mineralization is interpreted to have been stratabound and post-Tabberabberan.

Pyrite occurs as a lining in fractures and cavities, disseminated in dolostone, and as cylindrical growths <1 cm in diameter with galena. The cylindrical pyrite growths may be up to several centimetres in length and generally consist of a central core containing framboids, followed by radiating, strongly anisotropic pyrite surrounded by an outer rim of intergrown galena, sphalerite and barite (Fig. 4a). This pyrite is extremely porous, particularly within the core.

Galena occupies fractures cutting pyrite and occurs as infillings or possible replacements in the cores and rims of the cylindrical features (Fig. 4a). Galena contains rare inclusions of possible tetrahedrite, but these were too small to confirm by microprobe. Minor sphalerite with intergrowths of chalcopyrite is also found along the rims of cylindrical pyrite growths. Cavities and carbonate veins are commonly lined with well zoned non- to bright luminescent saddle dolomite locally accompanied by minor crystalline barite and later non-ferroan calcite. Zonation within sparry dolomite is related to variations in iron content, as discussed more fully in a subsequent section. The precipitation of galena and sphalerite was in part contemporaneous with the precipitation of saddle dolomite and barite. Supergene cerussite, smithsonite and chalcedonic quartz are also abundant.

Hume Park occurrence

The Hume Park occurrence is hosted by an isolated sliver of basal Buchan Caves Limestone located approximately 5 km east-northeast of Buchan on the west bank of the

Fig. 4 Photomicrographs showing textural features of pyrite. Scale bar bottom left of each photograph is 0.1 mm. (a) Cylindrical pyrite (py) from the Back Creek occurrence. Note the porous nature, bladed crystal habit, and anisotropy of the pyrite, suggesting that it was initially precipitated as marcasite. Galena (gn) is also present within the cylindrical structure as well as intergrown with saddle dolomite cement (dark). (b) Brecciated, colloform pyrite (py) from the McRae's limonite deposit. Note the porous nature of the pyrite and the colloform banding. Breccia fragments are cemented by calcite (dark).

generally occlude the remaining voids and occupy fractures cutting sphalerite. Late fractures containing intergrown quartz and calcite also cut sphalerite bands.

Spring Creek occurrence

The Spring Creek occurrence is located in the Caves Reserve approximately 2 km southwest of Buchan (Fig. 1) and is the only known base-metal occurrence hosted by the Buchan Caves Limestone on the western margin of the Buchan–Murrindal Synclinorium. Only a small amount of copper ore is reported to have been recovered from this occurrence and little information can be obtained from the former workings which consist of a vertical shaft and an adit driven southwest from the bank of Fairy Creek. These workings are now only partly accessible. Most of the copper mineralization is reported to have been restricted to the Spring Creek Member (Cochrane 1982), although this could not be confirmed by the present study. Despite the limited extent of the former workings, the Buchan Caves Limestone is well exposed in the area (see Fig. 6).

The Buchan Caves Limestone strikes north–south in the Caves Reserve and dips 30–40° to the east. The contact with the overlying Pyramids Marlstone Member has been offset along a major north to northwest-trending, steeply dipping reverse fault. Minor east-trending faults also displace the contact between the Buchan Caves Limestone and the overlying Pyramids Marlstone Member, as well as the contact between dolomitized and undolomitized Buchan Caves Limestone. Aside from a zone approximately 10 m thick underlain by a further 10 m thickness of Spring Creek Member, the basal 70 m of the Buchan Caves Limestone is pervasively dolomitized.

No sulphide minerals were identified in the former workings at Spring Creek, or in the mullock pile beside the vertical shaft, although minor malachite and azurite associated with several generations of carbonate veining

Murrindal River (Fig. 1). Exposure is poor in this area and a detailed map and stratigraphic section were not prepared for this occurrence. Hume Park was worked briefly in the 1870s and the best grade ore was reported to occur in a breccia adjacent to a west-dipping fault (Teichert & Talent 1958; Cochrane 1982). Most of the former workings are now inaccessible, although sulphide minerals may be observed at the adit entrance.

Sulphide minerals at Hume Park occur within a brecciated dolostone horizon 1–1.5 m thick subparallel to bedding and thus are locally strata-bound. Galena and sphalerite occur as fracture fillings, cavity linings and veinlets 1–10 mm thick parallel to bedding. Sphalerite commonly displays a well developed colour zonation where it lines cavities in which an initial band of red-coloured colloform sphalerite 1–2 mm across intergrown with minor galena is overgrown by crystalline yellow sphalerite (Fig. 5). Accessory pyrite occurs finely disseminated in the host dolostone and is also intergrown with sphalerite. Sparry dolomite and non-ferroan calcite

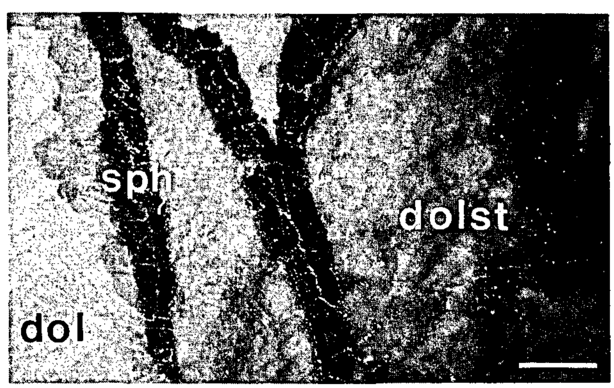

Fig. 5 Zoned sphalerite (sph) rimming cavities in dolostone (dolst) at the Hume Park occurrence. Scale bar in the bottom right corner is 2 mm. Sphalerite colour varies from dark red (>0.4 wt% Fe) to yellow (<0.4 wt% Fe). White sparry dolomite (dol) and calcite cement occlude the remaining cavity space.

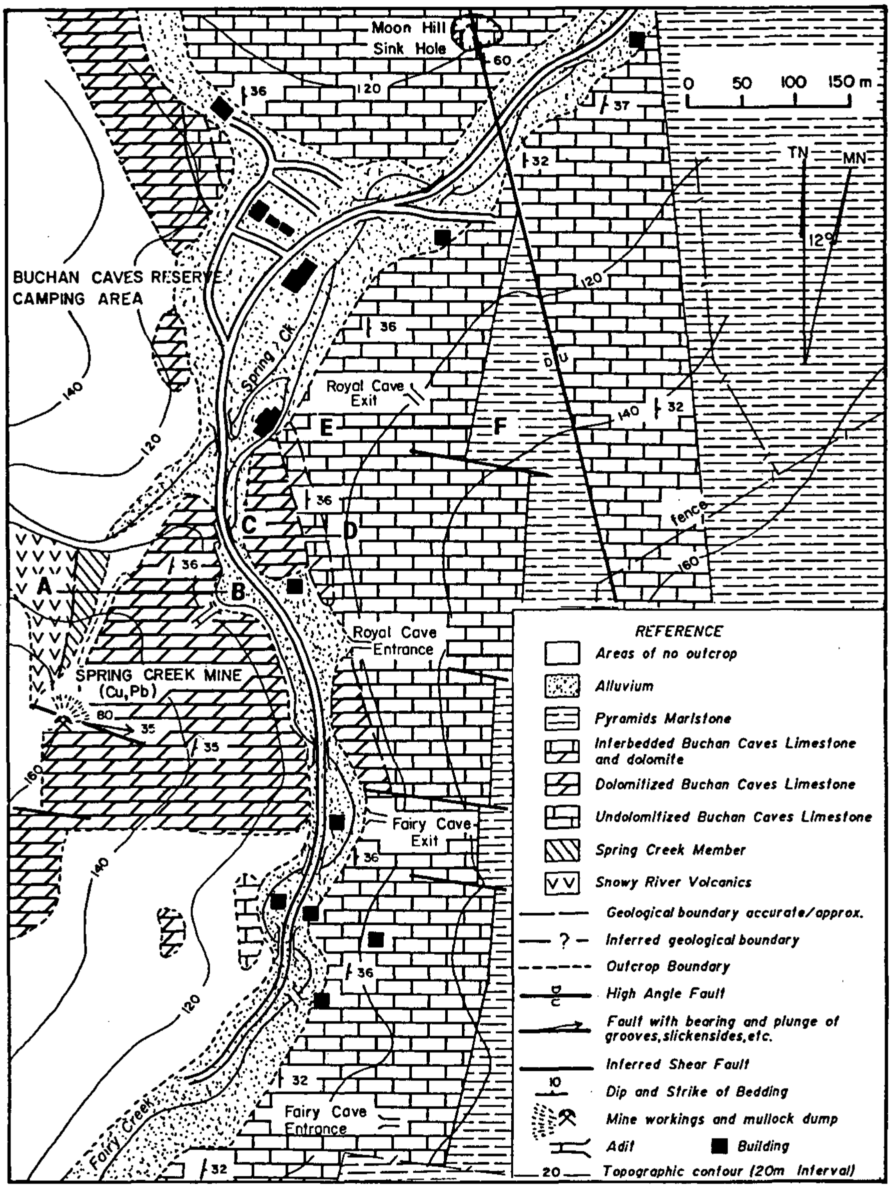

Fig. 6 Geological map showing the location of the Spring Creek occurrence (after Cromie 1990). A–F are the positions of measured stratigraphic sections shown in Fig. 7.

are present. Malachite also occurs along an east-southeast trending oblique slip fault exposed at the site of the former shaft and appears to post-date quartz slickenfibers developed along the fault surface. This fault is orientated subparallel to the east-trending faults described in the preceding paragraph, which are in turn subparallel to a major joint set in the Buchan Caves Limestone, suggesting that former joint planes were activated during faulting. Minor purple fluorite, similar to that observed near the Pyramids occurrence, also occurs associated with minor calcite veining in dolostone nearby.

McRae's limonite deposit

The McRae's limonite deposit is situated approximately 7 km south of Buchan (Fig. 1). It is hosted by limestone equivalent to the Murindal Limestone (Pype 1992) but which is much lighter in colour, and is one of several oxidized occurrences collectively known as McRae's limonite horizon (O'Shea 1980). Bowen (1970) described McRae's limonite deposit as stratiform and it is reportedly associated with a volcaniclastic horizon (O'Shea 1980), although on the basis of preliminary drilling results, Teichert and Talent (1958) considered the deposit to be irregular and wedge shaped and reported no tuffaceous material. The deposit is poorly exposed at surface but has been penetrated by several drill holes. Reserves of 6.8 Mt of 32% iron have been estimated (Bowen 1970). Samples of drill core were collected from two drill holes, TDH 32 and 33A.

A limestone drill core sample from above McRae's limonite horizon at a depth of 66 m in TDH 32 contains irregular cavities and carbonaceous stylolites lined with colloform pyrite. A later filling of ferroan calcite coats this pyrite as well as replacing fossils in the limestone host. Non-ferroan calcite fills the remaining cavity space, including apparent pressure shadows and forms fine veinlets which crosscut all previous phases.

McRae's limonite horizon was intersected between a depth of 153 and 193 m in TDH 32 where it contains irregular colloform pyrite bands 2–10 mm thick lining cavities 5–30 mm across within a bioclastic limestone. These cavities are orientated oblique to bedding in the host limestone and, after pyrite, are filled progressively with dull luminescent zoned calcite. The colloform pyrite is commonly cut by fracture fillings of non-ferroan calcite cement. Pyrite also occurs finely disseminated within the host rock. Minor sphalerite and galena occur as veins which appear to post-date the colloform pyrite.

Samples of partially dolomitized peloidal limestone from beneath the volcaniclastic horizon reported in TDH 33A contain approximately 1% pyrite which occurs as irregular patches 5–15 mm across. These patches post-date two earlier generations of ferroan calcite which pre-date stylolitization, but were followed progressively by sparry dolomite, ferroan calcite and non-ferroan calcite. An examination of drill core between a depth of 200 and 210 m indicates that dolostone is interbedded with a poorly sorted pebble conglomerate containing clasts of rhyolite. No true pyroclastic material was observed over this interval, which is all that is available of the volcaniclastic interval described in company reports.

Summary of occurrences

A number of common features can be identified from an examination of the six occurrences. Sulphide minerals are generally hosted by, but not restricted to, dolostone and appear to post-date dolomitization as well as an early generation of carbonate cements. The main phase of sulphide mineralization was closely associated with structural features of inferred Tabberabberan age, which it appears to have post-dated in most cases, and a dolostone horizon situated ~30 m above the base of the Buchan Caves Limestone (Fig. 7). An exception to this general observation is found at McRae's limonite deposit where the presence of brecciated colloform pyrite (Fig. 4b) suggests pre-or syn-tectonic emplacement of some metals, although post-Tabberabberan reactivation of structures or localized solution collapse might also explain brecciation.

There are also consistencies in the mineral paragenesis of the different occurrences examined (Fig. 8). Marcasite, now inverted to pyrite (see following discussion), was typically the first sulphide phase precipitated, followed by galena, sphalerite, and minor cubic pyrite. Galena clearly replaced early iron sulphide at the Pyramids occurrence and occupies fractures within cylindrical pyrite at Back Creek. In most cases base-metal sulphide precipitation was followed by the formation of dull luminescent sparry or saddle dolomite and, rarely, barite. The remaining porosity was generally occluded by ferroan to non-ferroan calcite, and saddle dolomite locally associated with purple fluorite.

LABORATORY RESULTS

Mineralogical investigations

As described in the previous section, sphalerite from Hume Park varies in colour from dark red to pale green. In many carbonate-hosted ore deposits a similar colour variation can be related to variations in iron content (e.g. Arne *et al.* 1991) although an association with cadmium content has also been demonstrated (Hardy 1979). Furthermore, variations in the iron content of sphalerite can be used to demonstrate fluctuations in the aO_2 of a mineralizing fluid (e.g. Giordano & Barnes 1981) assuming constant temperature and supply of iron. Accordingly, the composition of sphalerite was determined for closely spaced microprobe spot analyses along

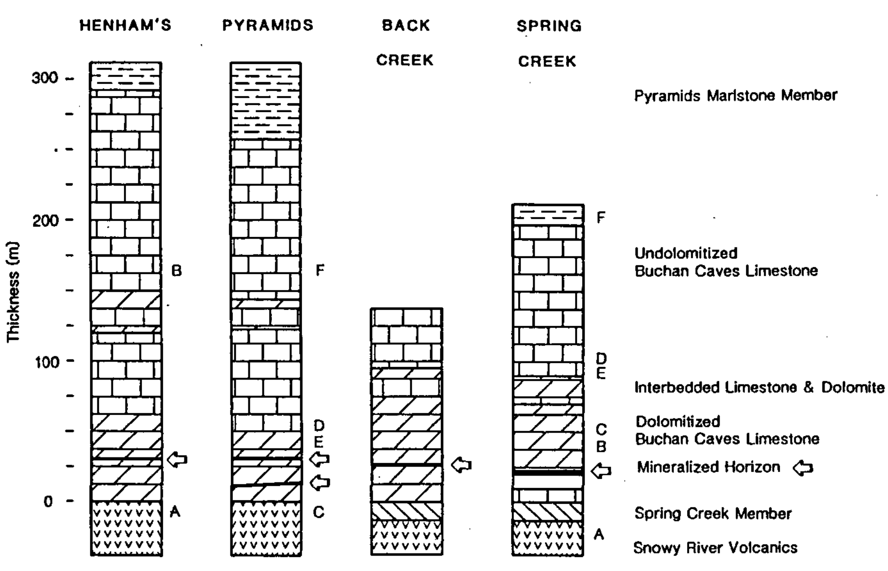

Fig. 7 Representative stratigraphic sections for the Henham's, Pyramids, Back Creek and Spring Creek occurences. The positions of the measured sections are shown in Figs 2, 3, and 6. Note that sulphide minerals are generally concentrated ~30 m above the base of the Buchan Caves Limestone, demonstrating the strata-bound nature of the occurrences.

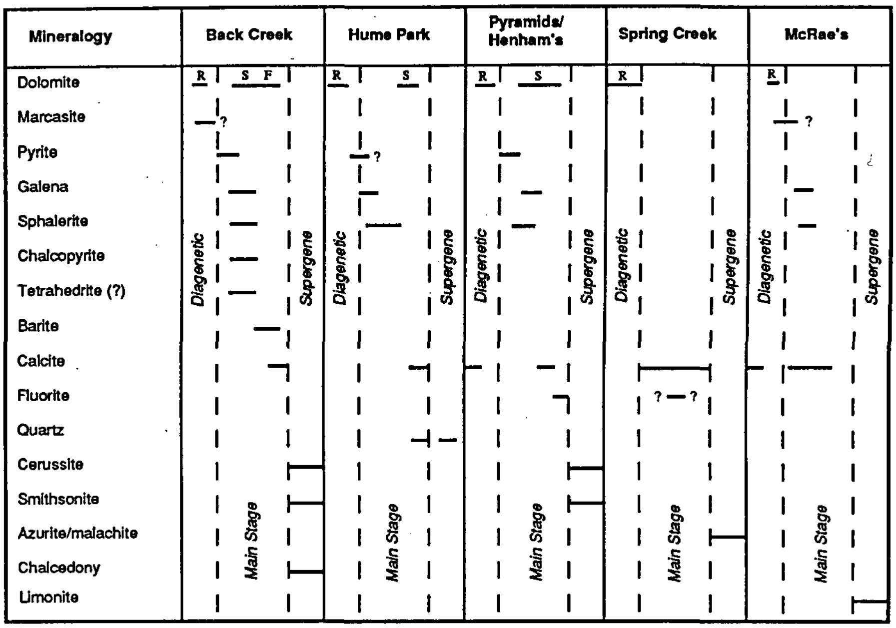

Dolomite phases: R - pervasive replacement of host rock by dolomite. S - saddle or sparry dolomite. F - ferroan dolomite

Fig. 8 Paragenetic summary for the Buchan Pb-Zn occurrences. Dolomite phases: R, pervasive replacement of host rock by dolomite; S, saddle or sparry dolomite; F, ferroan dolomite.

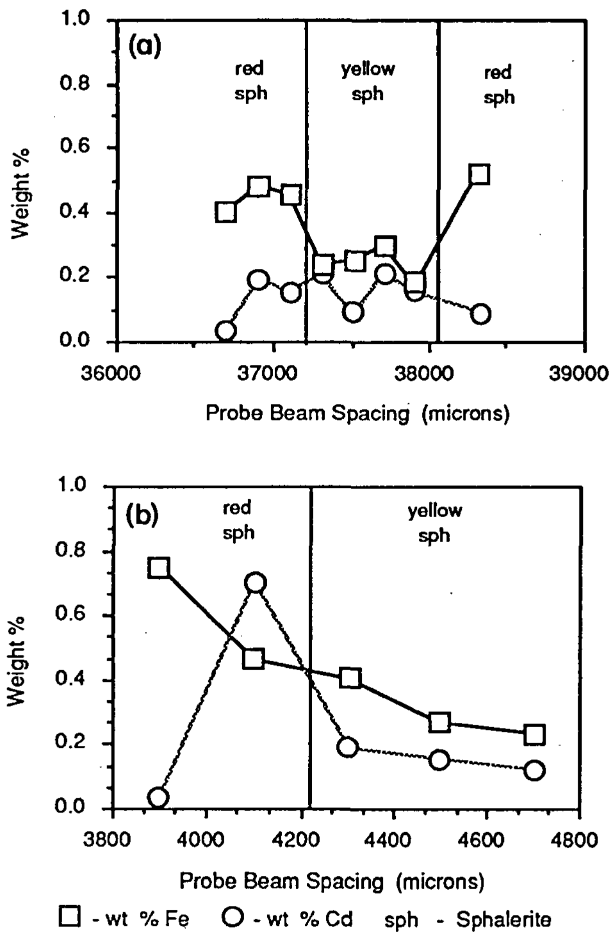

traverses perpendicular to colour zoning. The composition of pale green sphalerite from the Pyramids and Henham's occurrences was also determined.

The results of three representative traverses across colour-zoned sphalerite from Hume Park are presented in Table 1, along with the results of five analyses of sphalerite from the Pyramids and Henham's occurrences. Sphalerite from Hume Park shows a significant variation in iron content from 0.05 to 1.81 wt% which correlates with colour (see Fig. 9). Cadmium content varies from less than 0.07 wt% to 0.70 wt% but shows no consistent variation with colour (Fig. 9), although the highest value at Hume Park (0.70 wt%) correlates with red sphalerite in traverse b. Pale green sphalerite from the Pyramids, Henham's, and Back Creek occurrences has an iron content of 0.01–0.24 wt% that is similar to yellow sphalerite from Hume Park. However, the Cd content of sphalerite from the Pyramids and Henham's occurrences varies from 0.59 to 1.43 wt% and is consistently higher than the Cd content of sphalerite from Hume Park.

Six samples of anisotropic, bladed pyrite from the Back Creek occurrence, as well as colloform pyrite from McRae's limonite deposit, were examined by XRD analysis. These iron sulphide samples consist predominantly of pyrite, although minor diffraction lines characteristic of marcasite were also recognized. Given the porous

Fig. 9 Relationship between iron and cadmium contents with colour zonation in sphalerite from the Hume Park occurrence. (a) Traverse 1/8763-105. (b) Traverse 3/8763-105. Complete analyses from these traverses are given in Table 1. Sample numbers decrease from left to right. (□), wt % Fe; (O), wt % Cd; sph, sphalerite.

nature of the pyrite at Back Creek, as well as its bladed habit and marked anisotropy, it is probable that it has inverted from an original marcasite structure (Gait & Dumka 1986; Arne *et al.* 1991).

Microprobe analyses of carbonate cements reveal significant variations in iron content both between occurrences and within the paragenesis for individual occurrences. In general, dolomite cements from the Back Creek occurrence have the highest iron contents, with occasional Mg/Fe ratios <4.0 (i.e. ankerite). Carbonate cements from the Pyramids and Henham's occurrences generally contain <2 wt% $Fe(CO_3)$. The Fe/Mn ratios of the various carbonate cements vary from <1 to ~6, with the result that much of the carbonate cement gives a dull red luminescence. Where zonation in sparry dolomite from Hume Park is revealed by cathodoluminescence, this can be related to an increase in $Fe(CO_3)$ from <0.1 wt% in the cores of crystals to ~1.5 wt% near the margins, followed by a reduction in $Fe(CO_3)$.

Fluid inclusion microthermometry

Six samples containing transparent mineral phases associated with Pb and Zn sulphide minerals were selected for fluid inclusion analysis in order to estimate the temperature and salinity of the mineralizing fluid. Doubly polished thick sections from each sample were examined in detail, but suitable primary fluid inclusions were found in only two samples. Fluorite associated with carbonate-filled cavities from near the Pyramids occurrence contains numerous primary, two-phase fluid inclusions up to 20 μm in diameter, as well as secondary inclusions in well defined planes. Sphalerite from Hume Park contains rare primary two-phase inclusions less than 5 μm in diameter which were too small to be of use. However, a single primary fluid inclusion 12 μm across was located in late calcite that fills cavities lined with sphalerite from Hume Park.

The results of heating and freezing experiments performed on eight primary inclusions are listed in Table 2. Homogenization temperatures range between 160 and 212°C. As Th provides only a minimum estimate of the true trapping temperature, fluid temperatures

Table 1 Summary of sphalerite compositional data.

Analysis	Zn	Fe	Cd	S	Total
Hume Park occurrence (1/8763-105)					
1	67.30	0.52	0.10	31.36	99.28
2	66.50	0.17	0.16	31.54	98.37
3	66.89	0.30	0.21	31.20	98.60
4	67.81	0.25	0.08	31.54	99.68
5	67.07	0.24	0.20	31.57	99.08
6	67.72	0.45	0.15	31.21	99.53
7	66.85	0.48	0.19	31.71	99.23
8	66.44	0.40	ND	31.35	98.19
Hume Park occurrence (3/8763-105)					
17	66.10	0.23	0.12	31.64	98.09
18	66.26	0.26	0.15	31.44	98.11
19	66.75	0.40	0.19	31.17	98.57
20	66.18	0.46	0.70	31.03	98.37
21	65.84	0.74	ND	31.70	98.29
Hume Park occurrence (4/8663-7)					
22	65.88	0.66	0.09	31.54	98.17
23	65.05	1.81	ND	31.50	98.41
24	65.77	0.26	0.10	31.88	98.01
25	66.36	0.18	0.12	31.47	98.13
26	66.10	0.15	0.19	31.60	98.04
27	66.40	0.20	0.09	31.77	98.46
28	67.00	0.21	0.19	31.67	99.07
29	66.56	0.05	ND	31.51	98.17
Henham's occurrence (9073-28)					
45	65.81	0.08	1.19	31.19	98.27
46	66.31	0.05	0.66	31.03	98.05
47	66.50	0.24	0.59	31.42	98.75
Pyramids occurrence (8663-14)					
50	67.00	0.12	1.09	31.22	99.43
52	66.72	ND	1.43	31.17	99.32

All analyses are in wt%.
ND, not detected at a detection limit of 0.07 wt% for cadmium and 0.03 wt% for iron.
See Cromie (1990) for further analytical details.

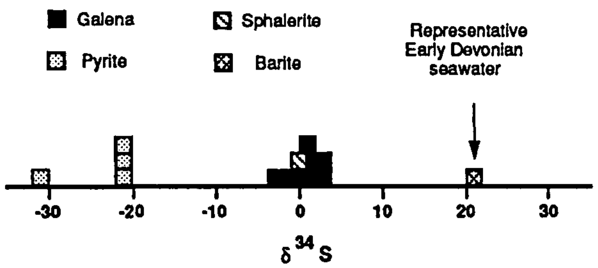

Fig. 10 Summary of sulphur isotope compositions of minerals from the Buchan sulphide occurrences. Shown are data given in Table 3 as well as data on three samples analysed at The University of Calgary. Representative Early Devonian seawater is taken from Claypool *et al.* (1980).

Table 3 Summary of sulphur isotope compositions.

Sample	Occurrence	Mineral	$\delta^{34}S$ (‰)
9073-1	McRae's limonite	Pyrite	-21.3
9073-2	Hume Park	Sphalerite	0.0
9073-3	Pyramids	Galena	+1.2
9073-4	Pyramids	Galena	+1.5
9073-5	Pyramids	Pyrite	-22.0
9073-6	Henham's	Galena	+4.1
9073-7	Henham's	Galena	-0.6
9073-8	Back Creek	Galena	-2.2
9073-9	Back Creek	Pyrite	-32.1
9073-10	McRae's limonite	Barite	+22.4

Analyses were performed by Kruger Enterprises Inc., Cambridge, Massachusetts, using Cañon Diablo troilite as a standard and a $^{34}S/^{32}S$ ratio of 0.0450045 (Ault & Jensen 1963). A standard error of ±0.05‰ is assumed.

associated with sulphide mineralization at Buchan were probably >160–212°C. Values of Tm determined from six of the inclusions range from -5.8 to -7.5, indicating fluid salinities of approximately 10 wt% NaCl equivalent.

Sulphur isotopes

The sulphur isotope composition of nine sulphide separates and a single barite separate were determined to place constraints on possible sulphur sources and mechanisms of sulphate reduction (Table 3). Given the very fine grained nature of sphalerite–galena intergrowths where the two phases co-exist, it was not possible to extract clean sphalerite and galena separates for paired isotopic determinations.

The sulphur isotope composition of three pyrite samples varies from -32.1 to -21.3‰. Five separates of galena gave $\delta^{34}S$ values ranging from -2.2 to +4.1‰, similar to a single value for sphalerite from Hume Park of 0.0‰. These results are similar to independent analyses of sulphide minerals from the Pyramids occurrence performed at the University of Calgary, Canada which gave values of +2.3‰ and +1.6‰ for galena, and an average value from three replicate analyses of -21.5±0.2‰ for pyrite. These results are summarized together with data from Table 3 in Fig. 10 which shows two distinct groupings of sulphur isotope compositions for pyrite and base-metal sulphide minerals from the Buchan occurrences. A single sample of barite from the McRae's limonite deposit gave a $\delta^{34}S$ composition of +22.4‰ that is similar to an average value for Early Devonian seawater in Australia (Fig. 10; Claypool *et al.* 1980).

Assuming that $\delta^{34}S$ values from pyrite are primary and have not been affected by inversion of marcasite to pyrite, the difference in sulphur isotope composition between pyrite and the base-metal sulphide minerals could not have been produced during equilibrium fractionation between coexisting sulphide phases, particularly at minimum temperatures for mineralization estimated to be in the range of 160–212°C (Ohmoto & Rye 1979). Therefore the observed spread in isotopic values indicates either non-equilibrium fractionation between coexisting

Table 2 Summary of fluid inclusion data.

Analysis	Mineral	Th (°C)	Tm (°C)	wt% NaCl eq.	Size (μm)
Pyramids occurrence					
1	Fluorite	160	-5.8	9	10
2	Fluorite	163	-6.6	10	12
3	Fluorite	185	*	—	<6
4	Fluorite	195	-5.6	8.8	12
5	Fluorite	197	-6.9	10.5	<6
6	Fluorite	205	-7.5	11.3	20
7	Fluorite	212	-6.0	9.4	12
Hume Park occurrence					
8	Calcite	195	*	—	12

Heating and freezing experiments were performed on a Linkam TH600 stage made available by BHP-Utah Minerals International, Hawthorn, Victoria with a precision of ±0.05°C (D. Gilbert, pers. comm. 1990).

* Freezing point depression not determined due to poor visibility.

Salinities were calculated using the equation of Potter *et al.* (1978) assuming a NaCl-H_2O system.

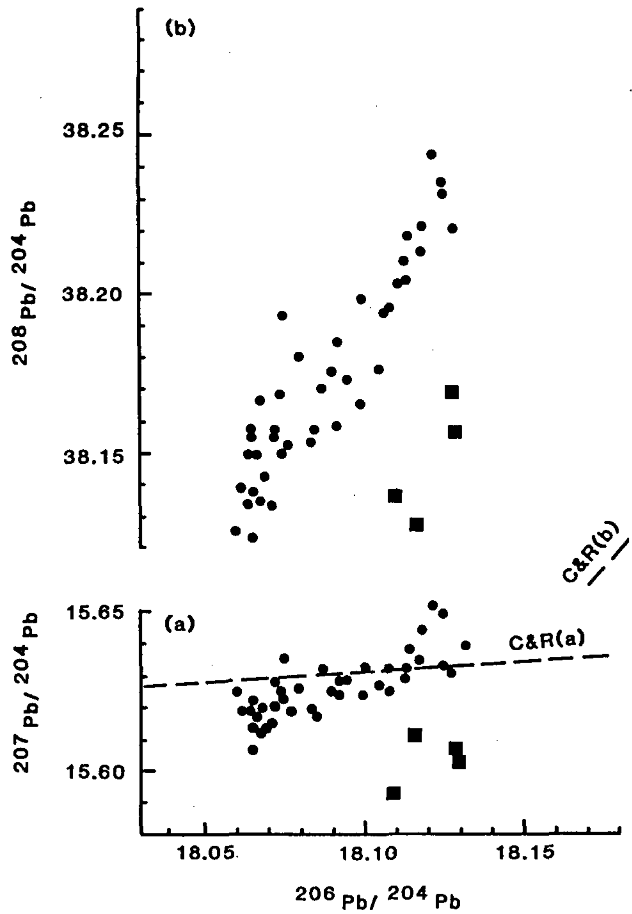

Fig. 11 Lead isotope composition of three galena samples from the Buchan occurrences (■) compared to the isotopic composition of lead from southeast New South Wales associated with Silurian magmatic activity (●). Also shown by dashed lines are the model 3 growth curves of Cumming and Richards (1975). Curve C&R (a), parameters U&Pb; curve C&R (b), parameters Th/U&Pb.

phases (e.g. bacterial sulphate reduction) or two separate mineralizing fluids. The involvement of bacteria during the precipitation of sulphides is precluded by the estimated temperatures of the mineralizing fluid (Trudinger *et al.* 1985), and therefore two distinct fluids are inferred for the Buchan sulphide occurrences. This conclusion is supported by the presence of an early generation of iron sulphide that generally appears to have preceded base-metal sulphides in all occurrences where they co-exist.

The ultimate source of sulphur is problematical. Barite from the McRae's deposit was presumably derived from Early Devonian seawater given their similar isotopic compositions. However, pyrite, and to a lesser extent galena and sphalerite, give isotopic compositions considerably less than Early Devonian seawater. The sulphur in pyrite could have been derived from seawater in a severely restricted marine basin or through bacterial reduction prior to heating of the mineralizing fluid (Ohmoto & Rye 1979). Sulphur in galena and sphalerite could also have been derived from seawater, particularly if sulphate reduction was incomplete (Ohmoto 1972). Alternatively, the sulphur in galena and sphalerite could have been derived from a primary magmatic source having an initial $\delta^{34}S$ close to zero per mil.

Lead isotopes

The lead isotope patterns for three Buchan galena samples are summarized in Table 4 and presented in Fig. 11 where they are compared with a representative Pb development (growth) curve (Model 3 of Cumming & Richards 1975) and with unpublished data from predominantly volcanic-hosted galena occurrences in southeast New South Wales. Lead isotope data from southeast New South Wales fit the model expectations well. In almost every locality galena is clearly associated with Silurian magmatic activity. The model ages range from about 450 to 410 Ma and the mean $\mu p = (^{238}U/^{204}Pb)_p$ at 10.74 ± 0.02 (s.d.) is very close to the growth-curve value of 10.75 ± 0.03 (s.d.), but the average source $Th/U = (^{232}Th/^{238}U)_p$ at 3.91 ± 0.01 (s.d.) is significantly higher than the growth-curve value of 3.84 ± 0.015 (s.d.). These data are similar in trend, without actually overlapping, to the Pb ratios in feldspars from Silurian granites in this region, recently reported by McCulloch and Woodhead (1993), whose interpretation applies equally well to these more precise galena results. The approximation to linear trends in each part of Fig. 11 is statistically significant, since the fractionation-error trends are shorter and much steeper.

From Fig. 11a it can be inferred that the hydrothermal solution(s) in New South Wales are 'crustal' in character, with a mean μ value almost exactly equal to the growth curve parameter. By contrast, the four Buchan values yield an average μp of 10.68 ± 0.02, more than two standard deviations below the (a) curve. The $(^{232}Th/^{238}U)_p$ value is also lower, at 3.88 ± 0.01, although still high compared with 3.84 of the relevant growth curve, which just appears at the lower right hand corner of Fig. 11b. The four filled squares show variation from locality to locality upon which is superimposed a modicum of measurement error. The two points on the left represent re-loads from the same solution of a sample from Back Creek. Their separation is within the expected analytical error of $\pm 0.03\%$ per mass unit, but the tie line between them is too steep for purely fractionation error. The two points to the right represent separate samples from the Pyramids–Henham's area. The separation between these two data-pairs reflects a possible geochemical difference between the samples, but the ratios are enough alike to permit averaging for the present discussion.

In the absence of lead isotope data from possible source rocks the interpretation of data from the Buchan occurrences must remain speculative. While the displacement between the Buchan and New South Wales data is small, it is large enough in terms of modern mass spectrometry to reveal that these data sets represent two distinct source regions. Low $^{207}Pb/^{204}Pb$ ratios (on the lower diagram) were associated by Russell (1972) with oceanic volcanic rocks. This correlation between low U/Pb and 'mafic' source rocks was subsequently systematized in the

Table 4 Galena Pb ratios and parameters.

Sample	Occurrence	$^{206}Pb/^{204}Pb$	$^{207}Pb/^{204}Pb$	$^{208}Pb/^{204}Pb$	$^{238}U/^{204}Pb_p$	$^{232}Th/^{238}U_p$
Pb269	Pyramids	18.129	15.602	38.157	10.68	3.88
Pb272	Pyramids	18.128	15.607	38.169	10.69	3.88
Pb271-1	Back Creek	18.116	15.611	38.127	10.70	3.87
Pb271-2	Back Creek	18.110	15.593	38.136	10.66	3.87
Model 3 parameters		—	—	—	10.75±0.03	3.84±0.02

Expected measurement precision (2σ) not greater than ±0.03%.

'Plumbotectonics' of Zartman and Doe (1981); more recent examples from Western Australia and South Africa have been summarized by Richards (1986).

Given the displacement of the Buchan data from the Fig. 11a growth curve, the calculation of model ages is tenuous. The isochron date, t_{76}, calculating to ~380 Ma, represents the intercept on the growth curve by the chord through meteorite and sample points. The data from the ^{206}Pb equation alone, t_6, at about 410 Ma, arises from the vertical projection of the sample point to the growth curve. Displacement on Fig. 11b is so large that model age calculation from the ^{208}Pb equation is pointless. Although the uncertainties associated with the data are large, the model ages are reasonably consistent with an Early Devonian age for the source of lead.

PHYSICAL AND CHEMICAL CONDITIONS OF SULPHIDE MINERALIZATION

The minimum temperature of sulphide mineralization is estimated to be in the range of 160-212°C on the basis of fluid inclusion homogenization temperatures. Marcasite is considered to be unstable over geologic time periods at temperatures above ~160°C (Murowchick & Barnes 1986) and so its precipitation prior to the main-stage mineralizing event would explain its almost complete inversion to pyrite, as suggested on the basis of petrography. Much of the sparry dolomite in the Buchan occurrences displays curved crystal edges and is therefore of the saddle variety. Saddle dolomite is considered to form in the sedimentary environment at temperatures greater than ~60°C (Radke & Mathis 1980) and its presence provides further support for the temperatures of mineralization estimated for the Buchan occurrences.

From the preceding descriptions of individual occurrences the following generalized paragenetic sequence was determined: marcasite–galena±sphalerite± pyrite–dolomite±barite–calcite±fluorite±dolomite, although it should be borne in mind that there is overlap between different phases. If it is assumed that the temperature during mineralization was ~200°C, then the aO_2 and pH of the fluid may be approximated by the field shown in Fig. 12. For a sphalerite iron content <2 wt%, the log aS_2 of the fluid is constrained to be approximately −13 assuming equilibrium between coexisting sphalerite and minor pyrite at Hume Park. The decreasing iron content of sphalerite at Hume Park reflects a slight increase in the aS_2 of the mineralizing fluid that may be attributed to increasing aO_2 during mineralization assuming constant temperature, or to decreasing temperature assuming constant aO_2. Following the precipitation of sulphides, the aO_2 of the mineralizing fluid moved into the sulphate stability field where barite precipitated, as shown in Fig. 12.

The pH of the mineralizing fluid may be estimated from the stabilities of three distinct mineral phases in the Buchan occurrences. The precipitation of primary marcasite requires a pH of <5.0 at 75°C (Murowchick & Barnes 1986), and a similar pH limit may also be inferred at 200°C (Arne *et al.* 1991). Thus if iron sulphide was initially precipitated as marcasite, as previously suggested, then the earliest mineralizing fluid must have initially been below pH 5.0. Following the introduction

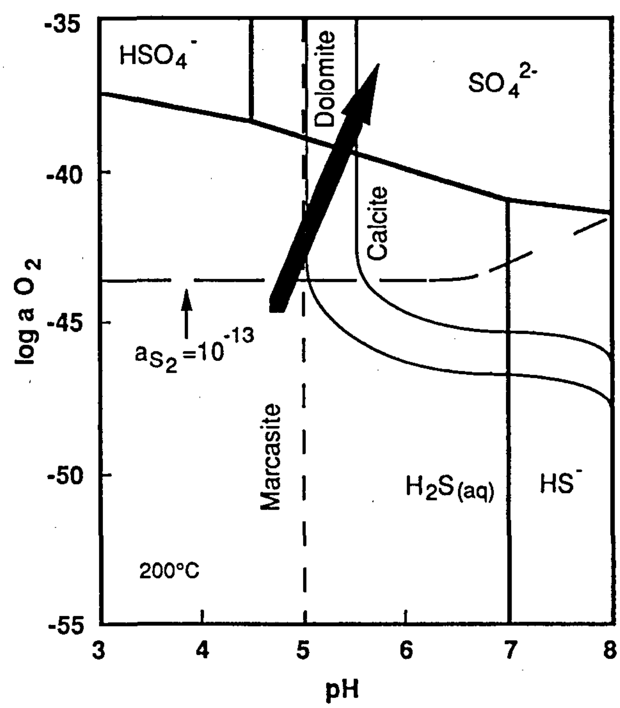

Fig. 12 Activity diagram inferred for the mineralizing solution at Buchan for 200°C. The generalized trend of the paragenetic sequence (heavy arrow) suggests increasing oxygen activity and pH for the mineralizing solution, although this does not preclude more than a single solution or minor reversals in the oxidation trend of the fluid. Modified from Arne *et al.* (1991). Carbonate mineral stabilities after Olson (1984).

of base metals, possibly by a second, separate mineralizing fluid, the pH moved into the stability field of dolomite and then calcite, as shown on Fig. 12. Therefore the overall trend of mineralizing fluids at Buchan was of increasing pH and aO_2. This is a generalized trend for sulphide mineralization at Buchan which does not preclude the involvement of more than one fluid and short-term reversals in the overall oxidation trend.

DISCUSSION

Genetic hypothesis

Barite from McRae's deposit is isotopically similar to Early Devonian seawater and, assuming that McRae's limonite horizon is cogenetic with sulphide occurrences stratigraphically lower in the Buchan Caves Limestone, it may be inferred that sulphur in the mineralizing fluid at Buchan was ultimately derived from seawater. The reduction of sulphur contained in pyrite probably involved bacteria, but this would not have occurred during base-metal mineralization as the estimated minimum temperatures were approximately 200°C. Therefore, sulphate incorporated into pyrite must have been reduced prior to heating of the mineralizing fluid, either in a distal sedimentary environment or in early diagenetic pyrite subsequently replaced by later iron sulphides, or else iron sulphide mineralization preceded the introduction of hot fluids. Sulphur incorporated into base-metal sulphides was derived from a separate solution which may have had a magmatic source or which may also have been derived from the reduction of seawater sulphate.

In the absence of a viable local heat source such as nearby intrusions, minimum temperatures during mineralization, inferred to have been in the range 160 to 212°C, require either a deep-seated fluid source, a relatively high geothermal gradient during shallow burial, or deep burial of the host sequence. An attempt to constrain the thermal history of the area through apatite fission track analysis of 11 samples of the Spring Creek Member and the Snowy River Volcanics met with failure due to a general absence of apatite in these rocks. A preliminary investigation of bitumen reflectance suggests that the Buchan Caves Limestone has been regionally heated to temperatures around 200°C (C. Barker pers. comm. 1992). Although the regional thermal history of southeastern Australia determined by Moore *et al.* (1986) suggests that the Buchan area has undergone substantial uplift and erosion since the mid to Late Cretaceous, regional temperatures of ~200°C immediately prior to Cretaceous cooling seem unlikely. Therefore it must be concluded that regional heating of the Buchan Caves Limestone occurred at some time between the Early Devonian and the Cretaceous although the mechanism for regional heating remains uncertain.

With regard to the origin of McRae's limonite horizon, it is of interest to note that occurrences associated with this horizon appear to be closely associated with the southern extension of the East Buchan Thrust (Fig. 1). At least one of these occurrences, Neils Creek, is hosted by a fault. These two observations suggest that McRae's Limonite Horizon may be structurally rather than stratigraphically controlled, consistent with the association of Pb–Zn mineralization with compressional structures noted for the five occurrences examined in detail.

As the Snowy River Volcanics directly underlie the Buchan Group, they are the most likely source of metals to evaluate. In particular, basaltic and epiclastic units provide readily leachable source rocks (Lydon 1986), and both occur in the Snowy River Volcanics (Orth *et al.* 1989). A source of metals from the underlying volcanics is also compatible with the lead isotope results which suggest a possible source of Early Devonian age which was somewhat depleted in uranium. It is therefore proposed that the metals may have been leached from the underlying Snowy River Volcanics by circulating saline fluids.

Whether the mineralizing solutions circulated through the Snowy River Volcanics within large convection cells (e.g. Russell 1986) or were expelled from confined aquifers (e.g. Lydon 1986) cannot be determined. However, it does appear likely that fluids migrated upwards along structures that were not established until the Middle Devonian Tabberabberan Orogeny. Faulting during the Tabberabberan Orogeny is largely concentrated in the basal portion of the Buchan Caves Limestone, and this may explain why carbonate strata higher in the sequence are generally less mineralized. Sulphide mineralization was not restricted to a single lithology (i.e. dolostone or limestone) although it is generally strata-bound, further suggesting that the main control on fluid migration was structural. The mechanism of sulphide precipitation remains conjectural, as it does in most carbonate-hosted base-metal occurrences, but the presence of organic material in the Buchan Caves Limestone, particularly concentrated along stylolites, may have aided the precipitation of sulphides, especially at the temperatures estimated for mineralization (e.g. Anderson 1991). Localization of sulphide mineralization ~30 m above the base of the Buchan Caves Limestone may either reflect enrichment in organic material at that particular stratigraphic level, such that sulphide minerals precipitated at the intersection of organic-rich horizons and faults, or the presence of early diagenetic marcasite at that particular horizon that could also have localized the precipitation of later base-metal sulphides.

Comparison with ore-deposit types

The sulphide occurrences hosted by the Buchan Group share several characteristics with typical Mississippi Valley-type (MVT) ore deposits (Anderson & MacQueen 1982; Mercer 1976). Sulphide mineralization at Buchan was clearly epigenetic, generally strata-bound, and was associated with, but not restricted to a dolostone host rock. The Buchan occurrences are mineralogically simple, and there is an obvious association between sulphide minerals and multiple generations of carbonate cement. Initial precipitation of marcasite is inferred at Buchan, and sphalerite from the occurrences also has a low iron content and cadmium contents typical of sphalerite from MVT deposits. Sparry dolomite, calcite, fluorite, and barite are also common in MVT deposits.

In addition to these similarities with MVT deposits, the Buchan occurrences also show features more characteristic of stratiform base-metal deposits (Gustafson & Williams 1981). Fluid inclusion homogenization temperatures in the range 160 to 212°C and fluid salinities of around 10 wt% NaCl eq. are, in general, more typical of stratiform ore deposits than of MVT deposits. Furthermore, the striking variation in sulphur isotope composition displayed by sulphide minerals from the Buchan occurrences is more typical of stratiform ore deposits, although some MVT deposits on the Lennard Shelf, Western Australia show similar characteristics (Lambert & Etminan 1987). In cross-section, the cylindrical pyrite from Back Creek is identical to pyrite spheroids identified in some stratiform Pb–Zn deposits from the Canadian Cordillera (Gu Lianxing & McClay 1992). The presence of detectable Ag, while not unknown in MVT deposits, is also more typical of stratiform ore deposits. In addition, the preliminary Pb isotope compositions of galena give a model Pb age similar to the stratigraphic age of the host sequence (e.g. Vassjoki & Gulson 1986).

Therefore, it appears that the Buchan sulphide occurrences share features typical of both MVT and stratiform ore deposits and are thus similar to base-metal deposits of Ireland hosted within Carboniferous strata (Hitzman & Large 1986). More specifically, the Buchan occurrences appear similar to the epigenetic footwall zone of the Silvermines deposit, with which it shares similar mineralogical, fluid inclusion, and sulphur isotope characteristics (Andrew 1986). However, the Buchan occurrences differ from the Irish deposits with regard to the important aspect of timing. The Irish deposits are considered to have formed during sedimentation in extensional basins in which fluid migration was largely facilitated along normal faults. Although the Snowy River Volcanics were formed in such an extensional setting, aside from coarse volcaniclastic material associated with McRae's limonite deposit, there is little evidence to suggest that extension continued through to Buchan Group sedimentation. Furthermore, sulphide mineralization appears to have been associated with structures inferred to be of Tabberabberan age, the effects of which were largely compressional in the Buchan area. Therefore, an 'Irish-style' of mineralization may not strictly be applicable for the Buchan occurrences.

CONCLUSIONS

Detailed investigations of minor base-metal occurrences hosted by the Lower Devonian Buchan Group near Buchan, Victoria indicate that the style of mineralization does not readily conform to characteristics typical of either Mississippi Valley-type or stratiform base metal deposits, although the occurrences are similar in some respects to the epigenetic zones of the Irish base-metal deposits hosted by Carboniferous rocks. A genetic hypothesis is proposed involving the circulation of a moderately saline fluid at minimum temperatures in the range 160 to 212°C through the underlying Snowy River Volcanics during or shortly after the Middle Devonian Tabberabberan Orogeny, with the precipitation of base-metal sulphide minerals localized within inferred Tabberabberan age structures.

ACKNOWLEDGEMENTS

First and foremost, we would like to thank BHP Minerals International for their generous support of this project. In particular, Dr Peter Gregory, Dave Gilbert and Fler Barlow were most helpful. Rimstone Cooperative provided a grant to P. Cromie to support field work in the Buchan area and this is gratefully acknowledged. The Victorian Department of Industry and Economic Planning and the Department of Conservation and Environment are thanked for allowing us to sample drill core material and to conduct field studies in the Spring Creek and Pyramids areas. Peter Jackson (La Trobe University) and Pat Kelly (Melbourne University) are thanked for their assistance with microprobe analyses. The lead isotope and some of the sulphur isotope data were obtained while J.R.R. was on leave at the Universities of Alberta (Edmonton) and of Calgary. Professors G. L. Cumming (University of Alberta) and H. R. Krouse (University of Calgary) are thanked for their hospitality, and assistance in many ways. The three sulphide samples analysed by J.R.R. were provided many years ago by Professors A. S. Buchanan and J. A. Talent. Malcolm Wallace is thanked for an initial review of the manuscript and Graham Carr and Ken McQueen provided helpful reviews.

REFERENCES

Anderson G. M. 1991. Organic maturation and ore precipitation in Southeast Missouri. *Economic Geology* **86**, 909–926.

Anderson G. M. & MacQueen R. W. 1982. Ore deposit models-6. Mississippi Valley-type lead-zinc deposits. *Geoscience Canada* **9**, 108–117.

Andrew C. J. 1986. The geology, structural setting and evolution of the Silvermines Pb–Zn deposits, Ireland. *In* Andrew C. J., Crowe R. W. A., Finlay S., Pennel W. M. and Pyne J. F. eds. *Geology and Genesis of Mineral Deposits in Ireland*, pp. 33-43. Irish Association of Economic Geologists, Dublin.

Arne D. C., Curtis L. W. & Kissin S. A. 1991. Internal zonation in a carbonate-hosted Zn–Pb–Ag deposit, Nanisivik, Baffin Island, Canada. *Economic Geology* **86**, 699–717.

Ault W. V. & Jensen M. L. 1963. Summary of sulfur isotope standards. *In* Jensen M. L. ed. Biogeochemistry of Sulfur Isotopes, National Science Foundation Symposium Proceedings, Yale University, New Haven.

Bowen K. G. 1970. Limonite at Buchan. *Mining and Geological Journal of Victoria* **6**, 71–79.

Cochrane G. W. 1982. Copper-lead-zinc and barium deposits of Victoria. *Geological Survey of Victoria Bulletin* **61**.

Claypool G. E., Hosler W. T., Kaplan I. R., Sakai H. & Zak I. 1980. The age curves of sulphur and oxygen isotopes in marine sulphate and their mutual interpretation. *Chemical Geology* **28**, 199–260.

Cromie P. 1990. Base metal occurrences of the Buchan Caves Limestone, Victoria. BSc(Hons) thesis, University of Melbourne, Melbourne (unpubl.).

Cumming G. L. & Richards J. R. 1975. Ore lead isotope ratios in a continuously changing Earth. *Earth and Planetary Science Letters* **28**, 155–171.

Ford D. C. & Williams P. W. 1989. *Karst Geomorphology and Hydrology*. Unwin Hyman, London.

Gait R. I. & Dumka D. 1986. Morphology of pyrite from the Nanisivik mine, Baffin Island, Northwest Territories. *Canadian Mineralogist* **24**, 685–688.

Giordano T. H. & Barnes H. L. 1981. Lead transport in Mississippi Valley type ore solutions. *Economic Geology* **76**, 2200–2211.

Gustafson L. B. & Williams N. 1981. Sediment hosted deposits of copper, lead and zinc. *Economic Geology 75th Anniversary Volume*, 139–178.

Gu Lianxing & McClay K. R. 1992. Pyrite deformation in stratiform lead–zinc deposits of the Canadian Cordillera. *Mineralium Deposita* **27**, 169–181.

Hardy J. L. 1979. Stratigraphy, brecciation and mineralization: Gayna River, Northwest Territories. MSc thesis, University of Toronto, Toronto (unpubl.).

Hitzman M. W. & Large D. 1986. A review and classification of the Irish carbonate-hosted basemetal deposits. *In* Andrew C. J., Crowe R. W. A., Finlay S., Pennel W. M. and Pyne J. F. eds. *Geology and Genesis of Mineral Deposits in Ireland*, pp. 217–238. Irish Association of Economic Geologists, Dublin.

Husain F. 1981. The geology and petrology of the Lower Devonian Buchan Group, Victoria. PhD thesis, University of Melbourne, Melbourne (unpubl.).

Lambert I. B. & Etminan H. 1987. Biogeochemistry and origins of sediment-hosted base-metal deposits. *Australian Bureau of Mineral Resources Yearbook*, 89–93.

Lydon J. W. 1986. Models for the generation of metalliferous hydrothermal systems within sedimentary rocks and their applicability to the Irish Carboniferous Zn–Pb deposits. *In* Andrew C. J., Crowe R. W. A., Finlay S., Pennel W. M. and Pyne J. F. eds. *Geology and Genesis of Mineral Deposits in Ireland*, pp. 555–577. Irish Association of Economic Geologists, Dublin.

McCulloch M. T. & Woodhead J. D. 1993. Pb isotopic evidence for deep crustal-scale fluid transport during granite petrogenesis. *Geochimica et Cosmochimica Acta* **57**, 659–674.

Mercer W. 1976. Minor elements in metal deposits in sedimentary rocks: A review of the recent literature. *In* Wolf K. H. ed. *Handbook of Strata-bound and Stratiform Ore Deposits 2*, pp. 1–27, Elsevier, Amsterdam.

Moore M. E., Gleadow A. J. W. & Lovering J. F. 1986. Thermal evolution of rifted continental margins: New evidence from fission tracks in basement apatites from southeastern Australia. *Earth and Planetary Science Letters* **78**, 255–270.

Murowchick J. B. & Barnes H. L. 1986. Marcasite precipitation from hydrothermal solutions. *Geochimica et Cosmochimica Acta* **50**, 2615–2629.

Ohmoto H. 1972. Systematics of sulfur and carbon isotopes in hydrothermal ore deposits. *Economic Geology* **67**, 551–578.

Ohmoto H. & Rye R. O. 1979. Isotopes of sulfur and carbon. *In* Barnes H. L. ed., *Geochemistry of Hydrothermal Ore Deposits*, pp. 509–561. Wiley and Sons, New York.

Olson R. A. 1984. Genesis of paleokarst and strata-bound zinc-lead sulfide deposits in a Proterozoic dolostone, northern Baffin Island, Canada. *Economic Geology* **79**, 1056–1103.

Orth K., Cas R. A. F. & Wright J. V. 1989. Facies analysis and facies associations in the recognition of volcanic centres in silicic terranes: An example from the Early Devonian of Australia. *Australian Journal of Earth Sciences* **36**, 167–188.

O'Shea P. J. 1980. Mineral potential of the Snowy River Volcanics and Buchan Caves Limestone. *Geological Survey of Victoria Report* **63**.

Potter R. W. II, Clynne M. A. & Brown D. L. 1978. Freezing point depression of aqueous sodium chloride solutions. *Economic Geology* **73**, 284–285.

Pype G. 1992. Geology of the South Buchan area, Victoria. BSc(Hons) thesis, La Trobe University, Melbourne (unpubl.).

Radke B. M. & Mathis R. L. 1980. On the formation and occurrence of saddle dolomite. *Journal of Sedimentary Petrology* **50**, 1149–1168.

Ramsay W. R. H. & Vandenberg A. H. M. 1986. Metallogeny and tectonic development of the Tasman Foldbelt system in Victoria. *Ore Geology Review* **1**, 213–257.

Richards J. R. 1986. Lead isotope signatures: Further examination of comparisons between South Africa and Western Australia. *Transactions of the Geological Society of South Africa* **86**, 285–304.

Russell M. J. 1986. Extension and convection: A genetic model for the Irish Carboniferous base metal and barite deposits. *In* Andrew C. J., Crowe R. W. A., Finlay S., Pennel W. M. and Pyne J. F., eds. *Geology and Genesis of Mineral Deposits in Ireland*, pp. 545–554. Irish Association of Economic Geologists, Dublin.

Russell R. D. 1972. Evolutionary model for lead isotopes in conformable ores and in ocean volcanics. *Reviews in Geophysics and Space Physics* **10**, 529–549.

Teichert C. & Talent J. A. 1958. The geology of the Buchan area. *Geological Survey of Victoria Memoir* **21**.

Trudinger P. A., Chambers L. A. & Smith J. W. 1985. Low temperature sulfate reduction: Biological versus abiological. *Canadian Journal of Earth Sciences* **22**, 1910–1918.

Vandenberg A. H. M. 1988. Silurian–Middle Devonian. *In* Douglas J. G. and Ferguson J. A. eds. *Geology of Victoria*, pp. 133–140. Geological Society of Australia, Melbourne.

Vandenberg A. H. M. & O'Shea P. J. 1981. Explanatory notes on the Bairnsdale 1:250 000 geological map. *Geological Survey of Victoria Report* **65**.

Vassjoki M. & Gulson B. L. 1986. Carbonate-hosted base metal deposits: Lead isotope data bearing on their genesis and exploration. *Economic Geology* **81**, 156–172.

Webb J. A., Fabel D., Finlayson B. L., Ellaway M., Li Shu & Spiertz H. P. 1992. Denudation chronology from cave and river terrace levels: The case of the Buchan karst, southeastern Australia. *Geological Magazine* **129**, 307–317.

Webb J. A., Finlayson B. L., Fabel D. & Ellaway M. 1991. The geomorphology of the Buchan karst: Implications for the landscape history of the Southeastern Highlands of Australia. *Special Publication of the Geological Society of Australia* **18**, 210–234.

Zartman R. E. & Doe B. R. 1981. Plumbotectonics — the model. *Tectonophysics* **75**, 135–162.

(Received 27 February 1992; accepted 21 June 1993)